Detailed comparison of hadronic and electronic models of gamma-ray origin in supernova remnant RX J1713.7-3946

V.N.Zirakashvili, F.A.Aharonian

Diffusive Shock Acceleration

Krymsky 1977; Bell 1978

Very attractive feature: power-law spectrum of particles accelerated, $\gamma=(\sigma+2)/(\sigma-1)$, where σ is the shock compression ratio, for strong shocks $\sigma=4$ and $\gamma=2$

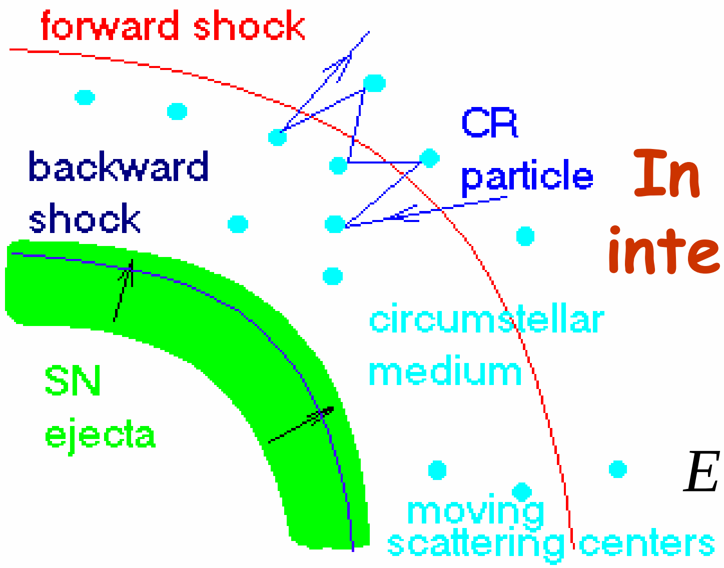

In the Bohm limit $D=D_B=cr_g/3$ and for interstellar magnetic field

$$E_{\max} = Z \cdot 10^{14}\,\mathrm{eV}\left(\frac{B}{10\,\mu\mathrm{G}}\right)\left(\frac{R_{\rm sh}}{3\,\mathrm{pc}}\right)\left(\frac{u_{\rm sh}}{3000\,\mathrm{km\,s^{-1}}}\right)$$

observations

radio emission

$\nu_{MHz} = 4.6\, B_{\mu G} E_{e,GeV}^2$

E = 50 MeV – 30 GeV

(100 GeV for IR)

$\gamma = 1.9 – 2.5$

$W_e = 10^{48} – 10^{49}$ erg

Ginzburg & Syrovatskii 1964

Shklovsky 1976

synchrotron

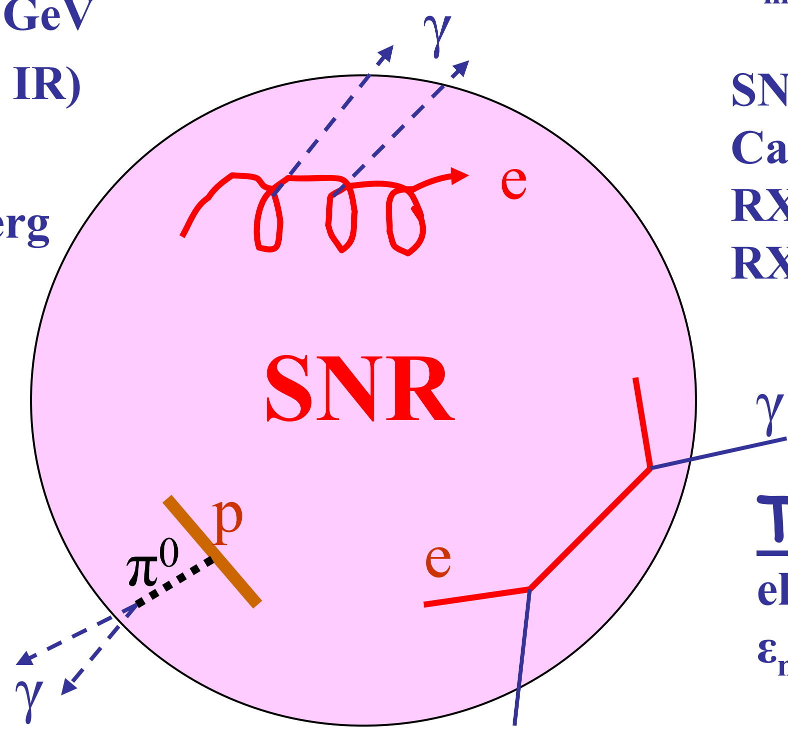

nonthermal X-rays

$\varepsilon_{keV} = 1\, B_{\mu G}(E_e/120\text{ TeV})^2$

$\varepsilon_{max} \sim 100$ TeV

SN1006 Koyama et al. 1995

Cas A Allen et al. 1997

RX J1713-39 Koyama et al. 1997

RX J0852-46 (“Vela jr”) Slane et 2001

inverse Compton

$\varepsilon_\gamma = \varepsilon_0(E_e/m_e c^2)^2$

TeV γ - rays

electrons/protons

$\varepsilon_{max} \sim 100$ TeV

confirmed by HESS (2008) !

SN1006 Tanimori et al 1998

RX J1713 Muraishi et al. 2000

Aharonian et al. 2004

Cas A Aharonian et al. 2001

RX J0852-46 (“Vela jr”)

G338.3-0.0; G23.3-0.3; G8.7-0.1…

Aharonian et al. 2005

γ-rays (π^0)

E = 30-3000 MeV

γ Cygni, IC443

Esposito et al. 1996

Sturner & Dermer 1996

Observations of RX J1713.7-3946: gamma-rays

Aharonian et al 2008 (HESS)

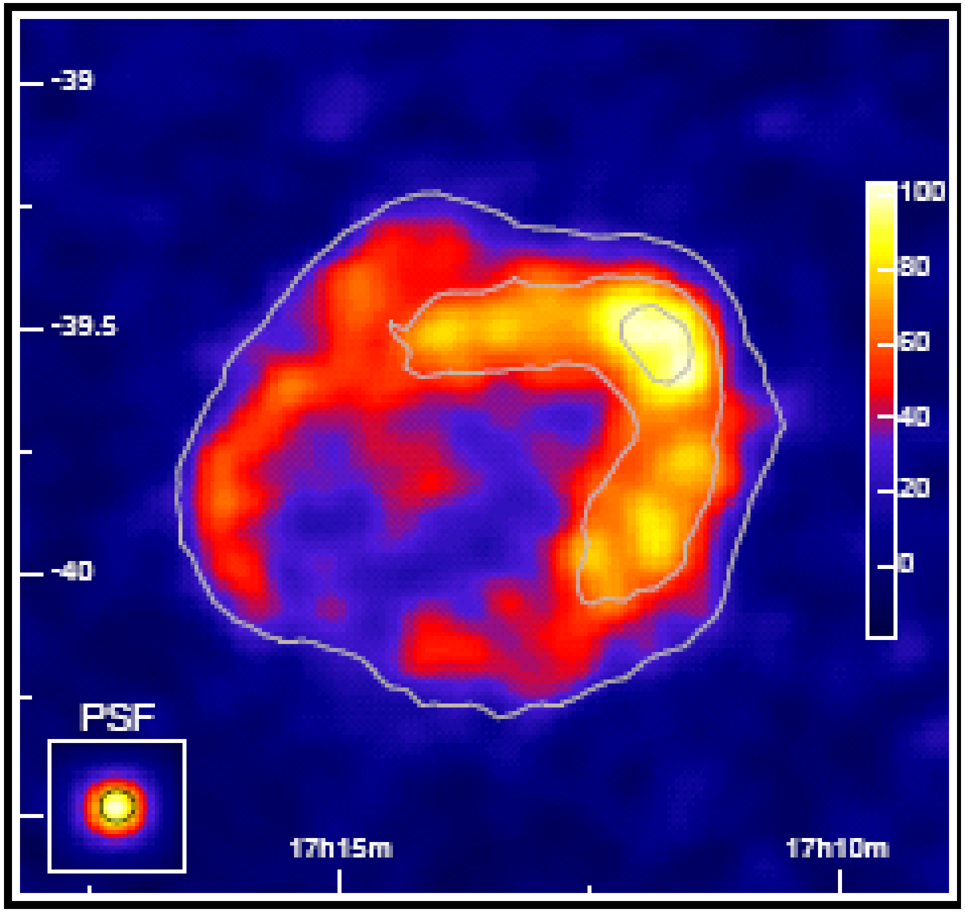

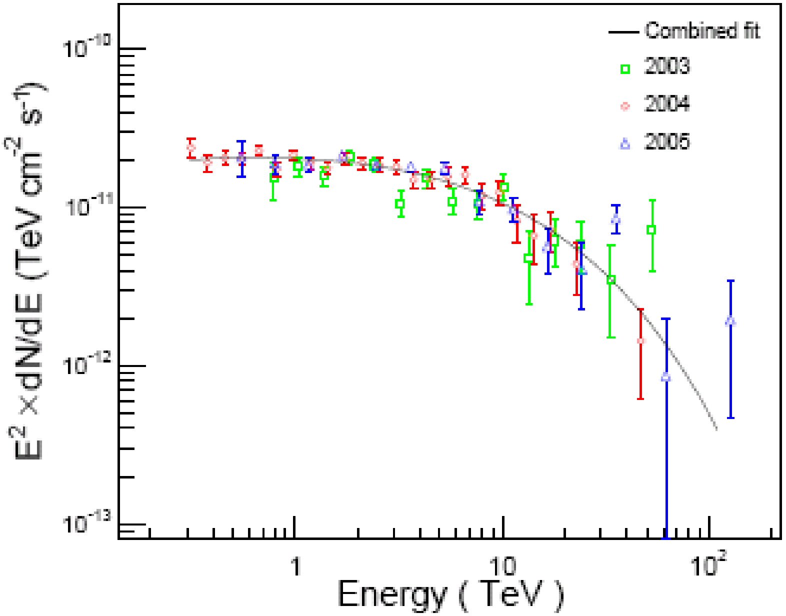

Radio-image (Lazendic et al. 2004)

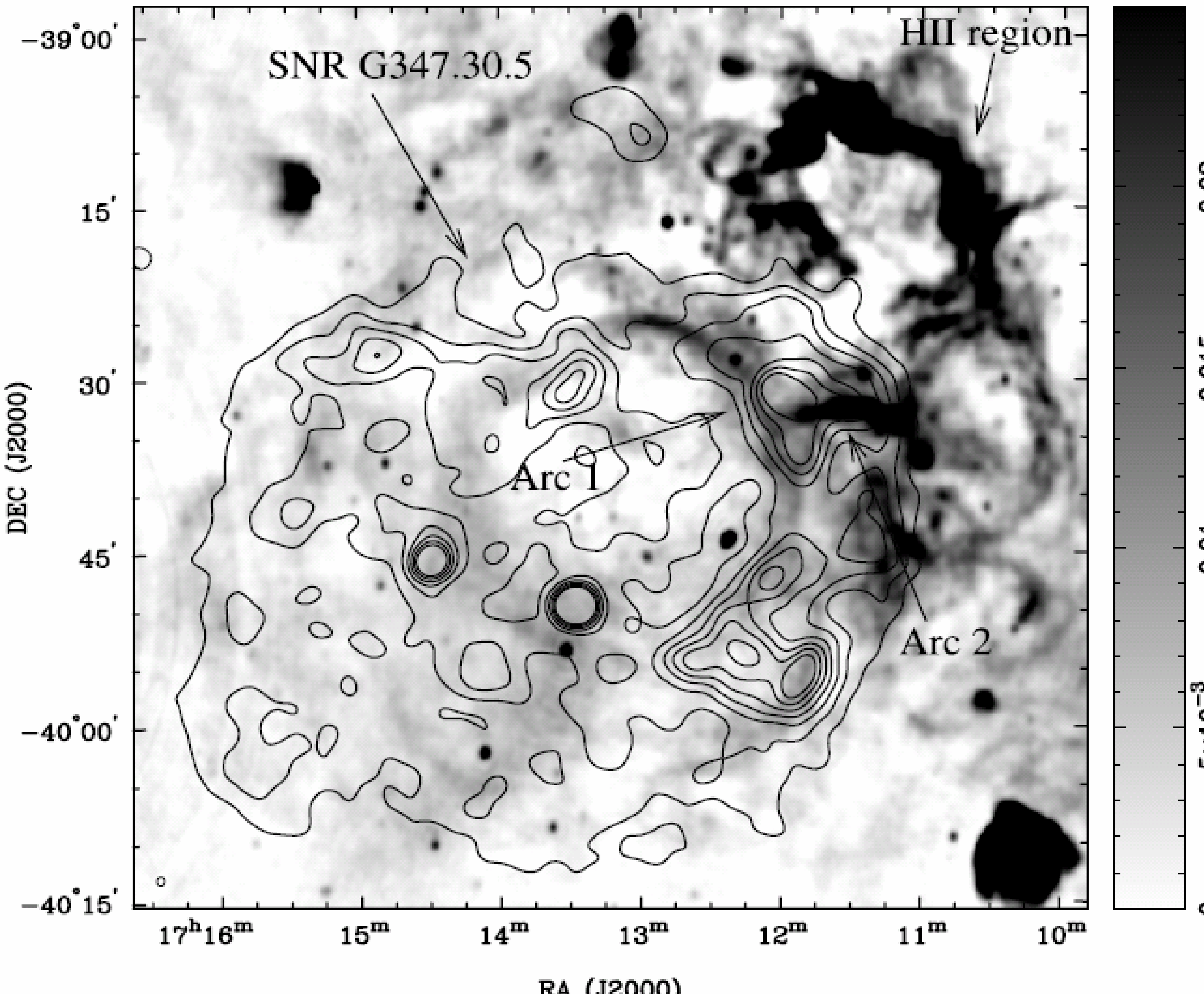

FIG. 5.—ATCA images of G347.3−0.5 and surrounding region at 1.4 GHz. The image was convolved with a Gaussian restoring beam of 46″ × 36″ (P.A. = −3°.8), shown by the tiny ellipse in the bottom left-hand corner. The image is overlaid with the *ROSAT* contours with the same levels as in Fig. 1. The linear gray scale is in units of Jy beam^{-1}.

X-rays: XMM-Newton, Acero et al. 2009

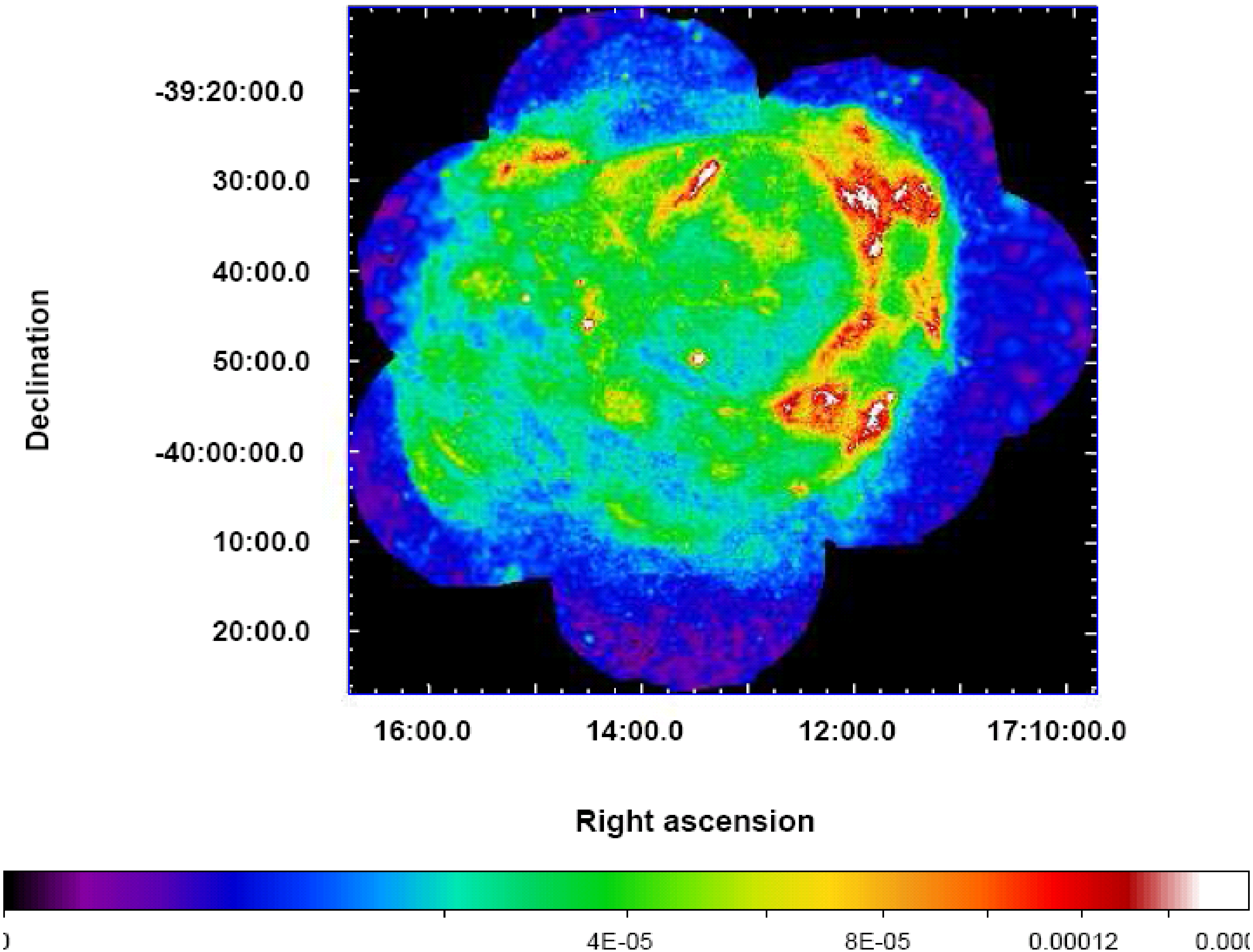

Fig. 1. EPIC MOS plus PN image in the 0.5-4.5 keV band. The units are ph/cm^2/s/arcmin^2 and the scale is square root. The image was adaptively smoothed to a signal-to-noise ratio of 10.

Comparison of gamma-ray and X-ray images

Tanaka et al. 2008
(Suzaku)

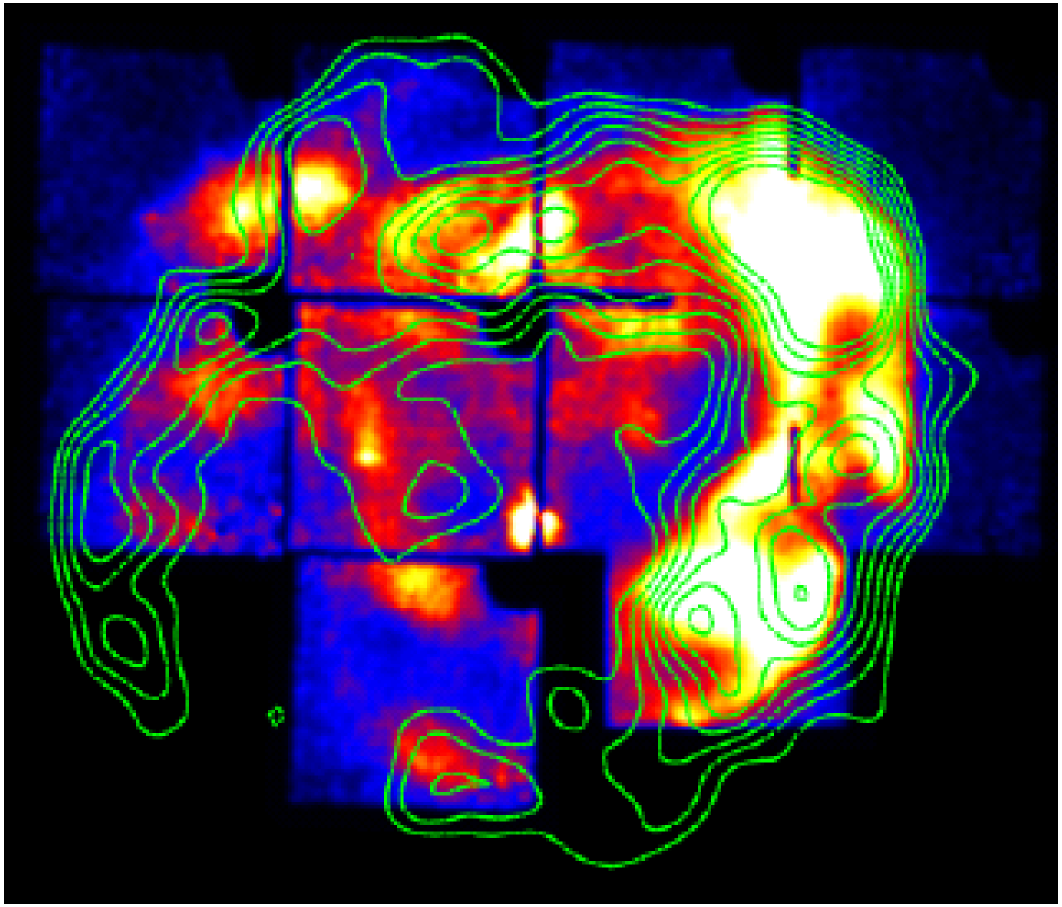

FIG. 8.— Comparison of the *Suzaku* XIS image and the gamma-ray image by the H.E.S.S. telescope (contours) taken from Aharonian et al. (2007) shown with color scale and green contours, respectively. The XIS image is same as Figure 7 (a) but the scale is changed to stress the similarity of the two images.

Correlation with molecular gas

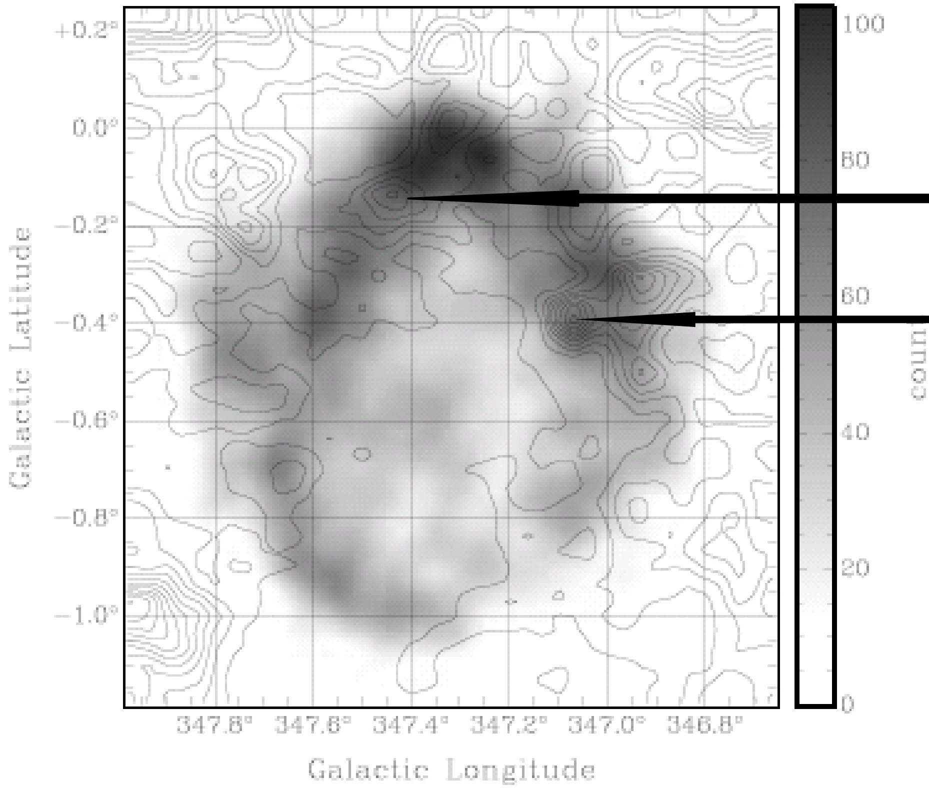

FIGURE 2. Gamma-ray image of G347.3-0.5 taken by HESS (Aharonian et al. 2007) in gray scale. Overlay map of G347.3-0.5 HESS image and ^{12}CO (J =1–0) intensity contours. The intensity is derived by integrating the ^{12}CO (J =1–0) spectra from −18 to 0 km s^{-1}. The lowest contour level and interval are 3 K km s^{-1} and 5 K km s^{-1}, respectively.

Fukui 2008

Cloud D -300 solar masses

Cloud C - 400 solar masses

Clouds C and D presumably swept up by the forward shock of the SNR

Estimated distance: D=6 kpc (Slane et al. 1999)

D=1 kpc (Fukui et al. 2003),
D=1.3±0.4 kpc (Cassam-Chenai et al. 2004)

AD393 in the ancient Chinese records (Wang et al.1997)

Age: 1600 yr

CR acceleration at the reverse shock? Seems presents in Cas A (Helder & Vink 2008)

Magnetic field of ejecta?

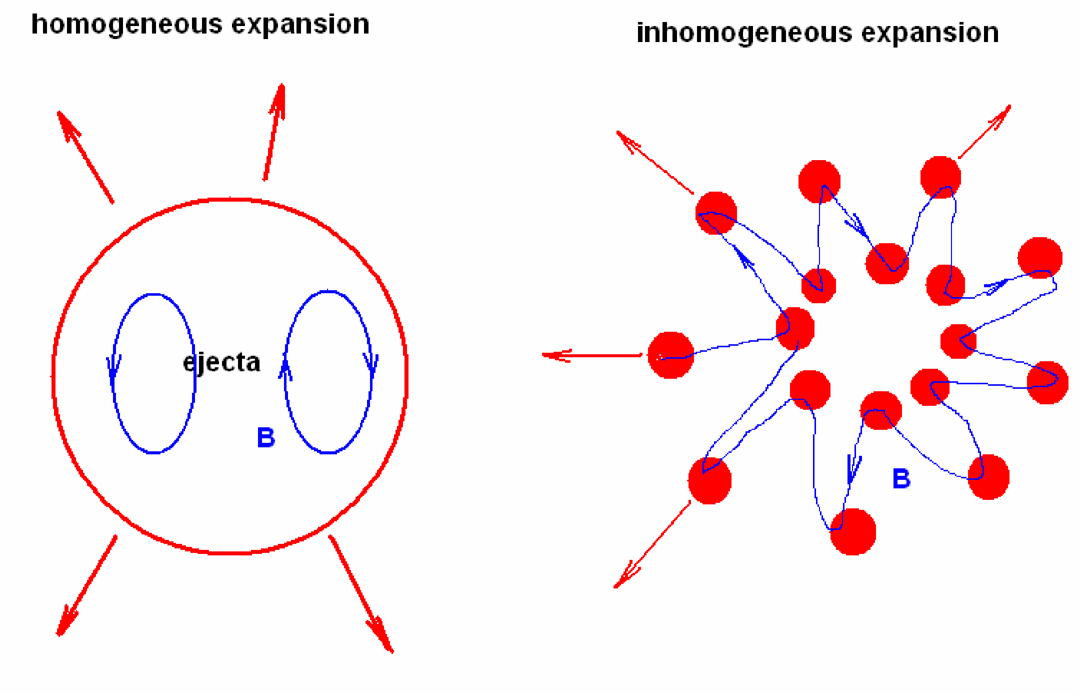

+additional amplification by the nonresonant streaming instability (Bell 2004)

$B \sim R^{-2}$, 100G at $R=10^{12}$ cm -

10^{-12}G at $R=10^{19}$cm=3pc

Field may be amplified and become radial – enhanced ion injection at the reverse shock

Numerical model of nonlinear diffusive shock acceleration

(natural development of existing models of Berezhko et al. (1994-2006), Kang & Jones 2006)

Spherically symmetric HD equations + CR transport equation

$$\frac{\partial \rho}{\partial t} = -\frac{1}{r^2}\frac{\partial}{\partial r} r^2 u \rho \quad (1)$$

$$\frac{\partial u}{\partial t} = -u\frac{\partial u}{\partial r} - \frac{1}{\rho}\left(\frac{\partial P_g}{\partial r} + \frac{\partial P_c}{\partial r}\right) \quad (2)$$

$$\frac{\partial P_g}{\partial t} = -u\frac{\partial P_g}{\partial r} - \frac{\gamma_g P_g}{r^2}\frac{\partial r^2 u}{\partial r} - (\gamma_g - 1)(w-u)\frac{\partial P_c}{\partial r} \quad (3)$$

$$\frac{\partial N}{\partial t} = \frac{1}{r^2}\frac{\partial}{\partial r} r^2 D(p,r,t)\frac{\partial N}{\partial r} - w\frac{\partial N}{\partial r} + \frac{\partial N}{\partial p}\frac{p}{3r^2}\frac{\partial r^2 w}{\partial r}$$
$$+ \frac{\eta_f \delta(p-p_f)}{4\pi p_f^2 m}\rho(R_f+0,t)(\dot{R}_f - u(R+0,t))\delta(r-R_f(t))$$
$$+ \frac{\eta_b \delta(p-p_b)}{4\pi p_b^2 m}\rho(R_b-0,t)(u(R_b-0,t) - \dot{R}_b)\delta(r-R_b(t)) \quad (4)$$

Minimal electron heating by Coulomb collisions with thermal ions

Numerical results

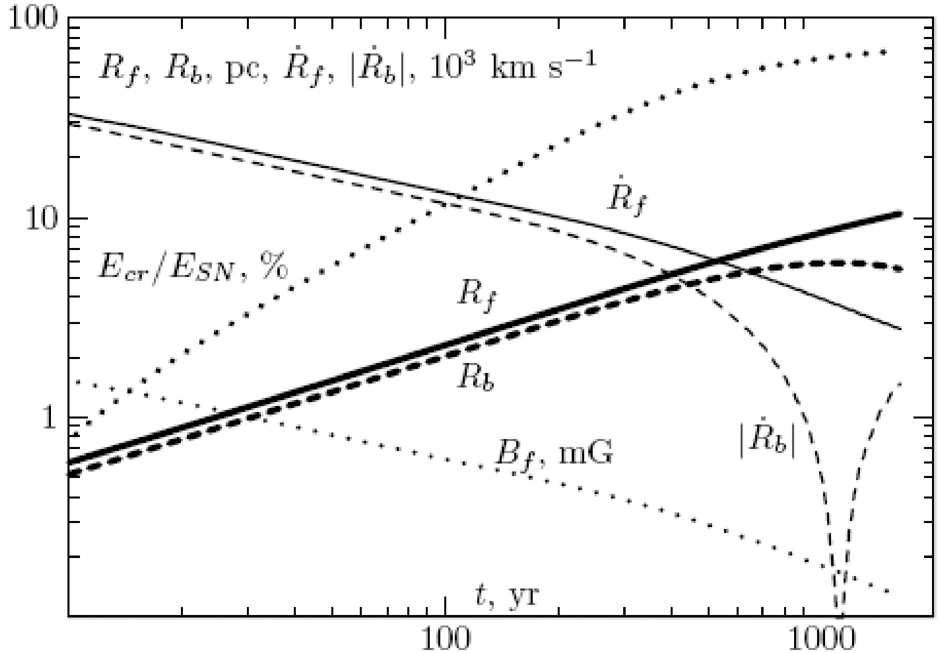

Fig. 1.— Time dependencies of parameters characterizing the forward and reverses shocks: the forward shock radius R_f (thick solid line), the reverse shock radius R_b (thick dashed line), the forward shock velocity $\dot{R}_f$ (thin solid line); the reverse shock velocity $\dot{R}_b$ (thin dashed line); the magnetic field strength downstream of the forward shock (thin dotted line); the ratio of the CR energy to the total energy of the supernova explosion E_{cr}/E_{SN} (dotted line).

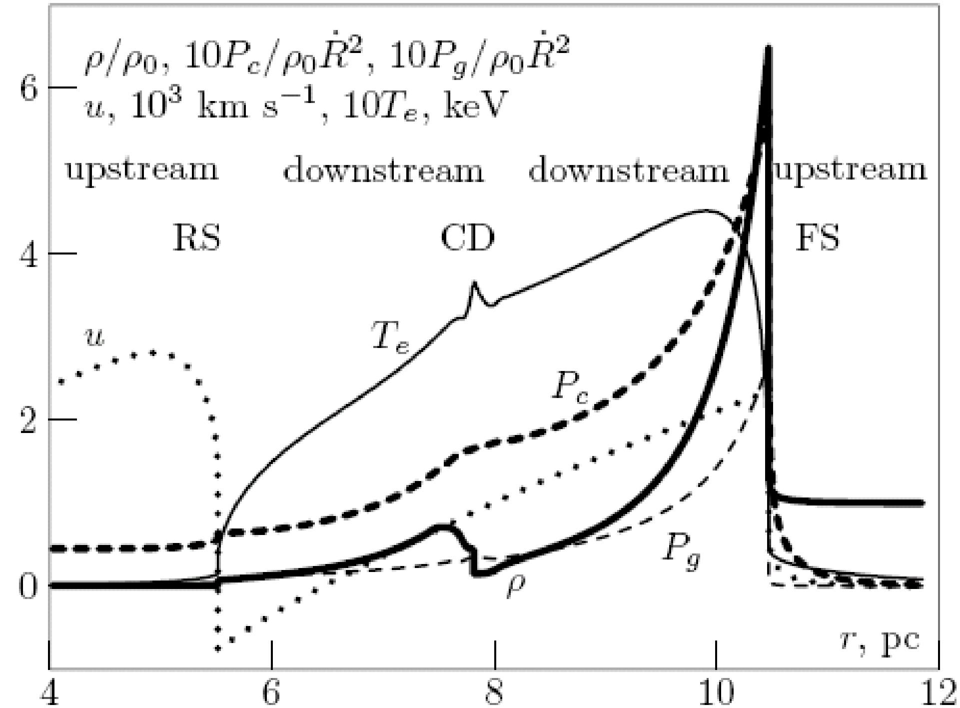

Fig. 2.— Radial dependencies of the gas density (thick solid line), the gas velocity (dotted line), CR pressure (thick dashed line), the gas pressure (dashed line) and the electron temperature (thin solid line) at $t = 1620$ yr. The calculations result in the following parameters in the present epoch: the forward shock velocity 2760 km s^{-1}, its radius 10.5 pc, the magnetic field strength downstream of the forward shock 127 μG. In the same figure we show the positions of the forward and reverse shocks, (FS and RS, respectively) and the contact discontinuity (CD).

Spectra of accelerated particles

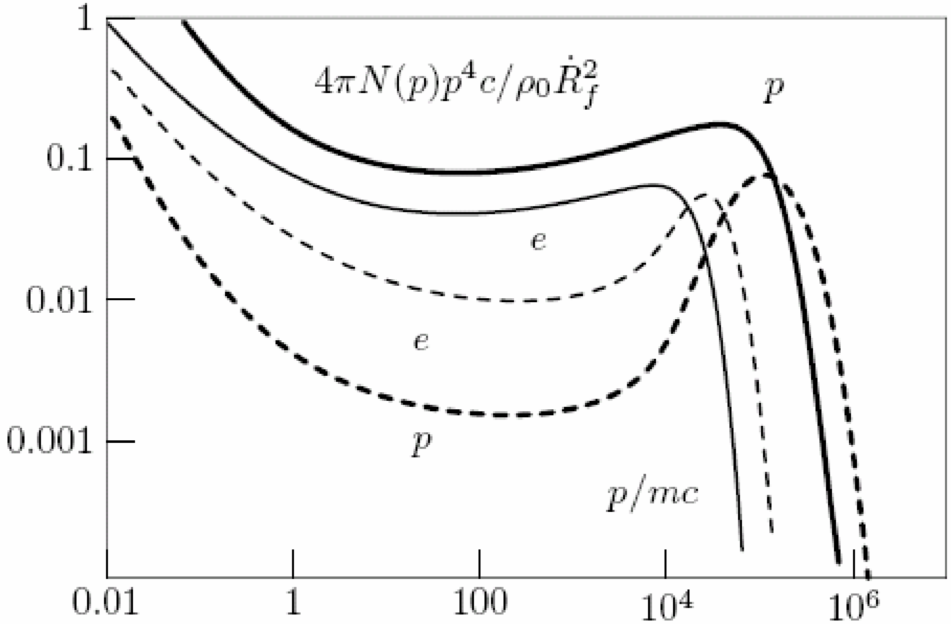

Fig. 3.— The energy distributions of accelerated protons (thick lines) and electrons (multiplied to the factor of 5000, thin lines) at the epoch $t = 1620$ yr. The spectra at both the forward shock (solid lines) and at the reverse shock (dashed lines) are shown.

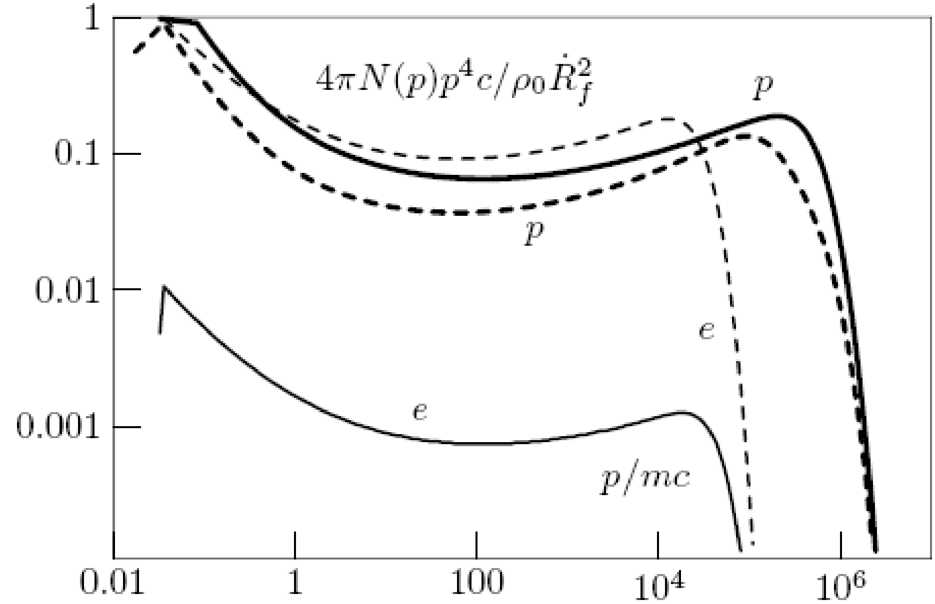

Fig. 4.— The energy distributions of accelerated protons (thick lines) and electrons (multiplied to the factor of 5000, thin lines) at $t = 100$ yr. Spectra at both the forward shock (solid lines) and the reverse shock (dashed lines) are shown.

Integrated spectra

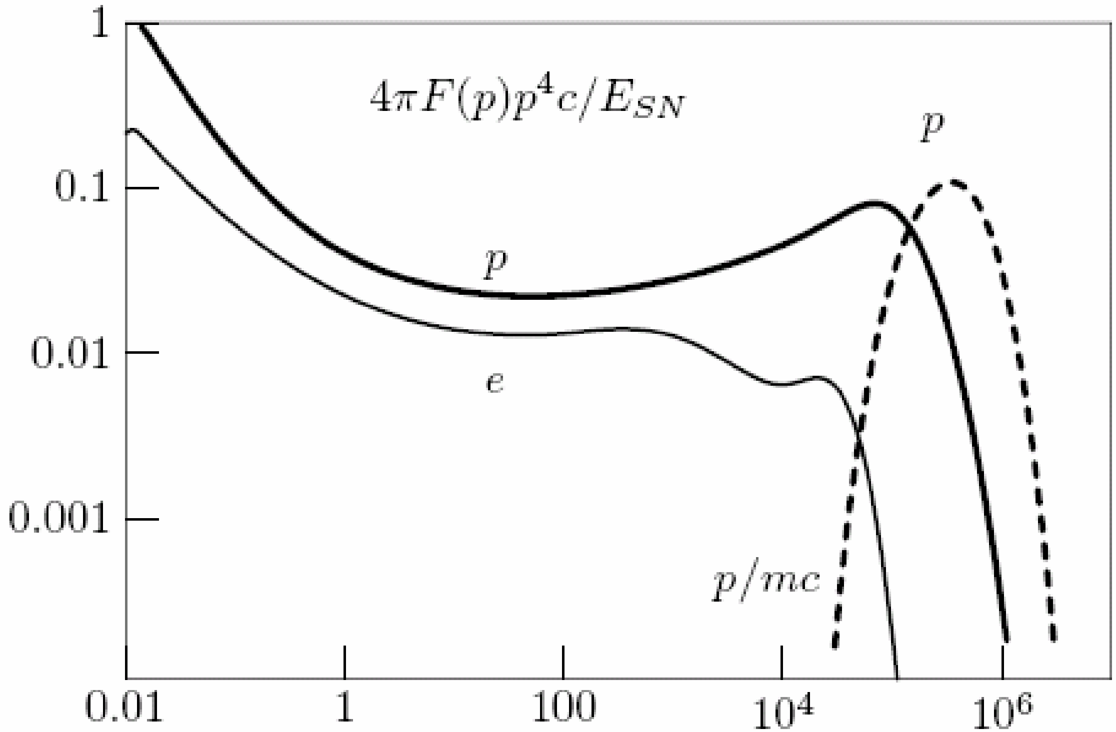

Fig. 5.— Spatially integrated spectra of accelerated protons (solid line) and electrons (multiplied to the factor of 5000, thin solid line) at $t = 1620$ yr. Spectrum of run-away particles which have left the remnant is also shown (dashed line).

E_{max}=800 TeV for this SNR in the hadronic model

Spectral modeling of RXJ1713.7-3946

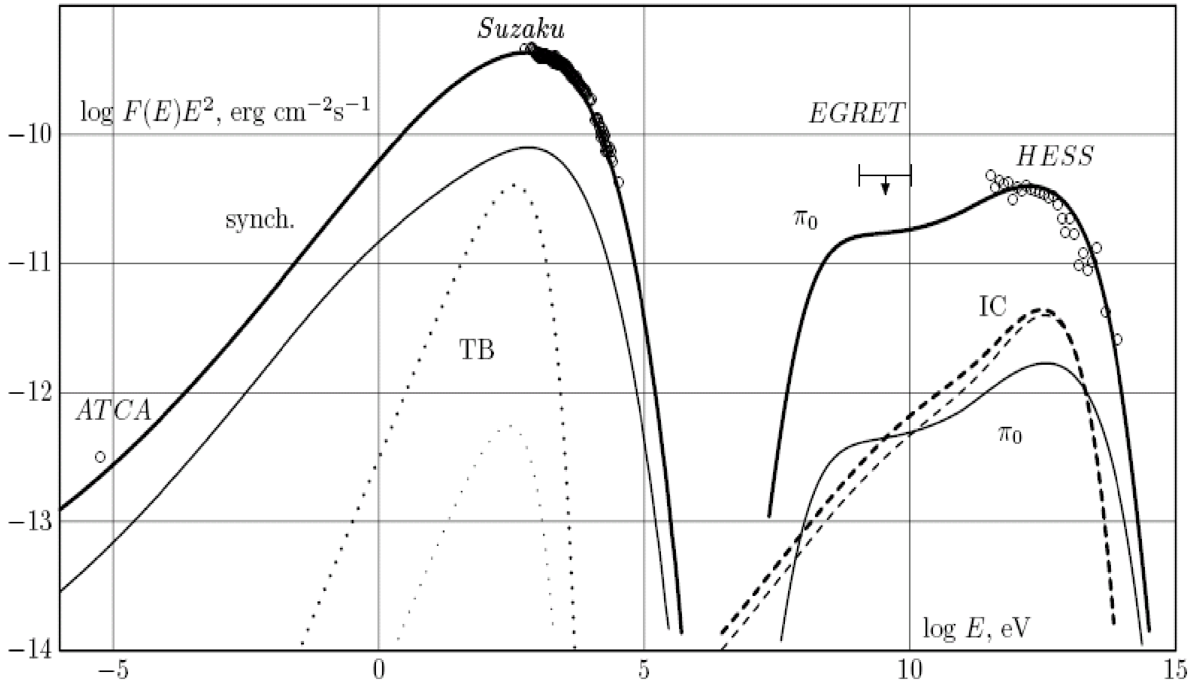

Fig. 6.— The results of modeling of of nonthermal radiation of RX J1713.7-3946 within the hadronic scenario of gamma-ray production. The following basic parameters are used: $t = 1620$ yr, $D = 1.2$ kpc, n_H =0.09 cm^{-3}, $E_{SN} = 2.7 \cdot 10^{51}$ erg, $M_{ej} = 1.5M_\odot$, $M_A^f = M_A^b = 23$, $\xi_0 = 0.05$, the electron to proton ratios at the forward and reverse shocks $K_{ep}^f = 10^{-4}$ and $K_{ep}^b = 1.4 \cdot 10^{-3}$. The calculations lead to the following values of the magnetic fields and the shock speeds at the present epoch: the magnetic field downstream of the forward and reverse shocks $B_f = 127$ μG and $B_b = 21$ μG respectively, the speed of the forward shock $V_f = 2760$ km s^{-1}, the speed of the reverse shock $V_b = -1470$ km s^{-1}. The following radiation processes are taken into account: synchrotron radiation of accelerated electrons (solid curve on the left), IC emission (dashed line), gamma-ray emission from pion decay (solid line on the right), thermal bremsstrahlung (dotted line). The input of the reverse shock is shown by the corresponding thin lines. Experimental data in gamma-ray (HESS; Aharonian et al. 2007a) and X-ray bands (Suzaku; Tanaka et al. 2008), as well as the radio flux 22 ± 2 Jy at 1.4GHz (ATCA; Acero al. 2009) from the whole remnant are also shown.

The main problem of hadronic origin of the gamma-rays of this supernova – absence of thermal X-ray emission (Katz & Waxman 2007). This gives an upper limit of circumstellar density only 0.02 cm^{-3} (Cassam-Chenai et al. 2004).

Leptonic model with a non-modified forward shock

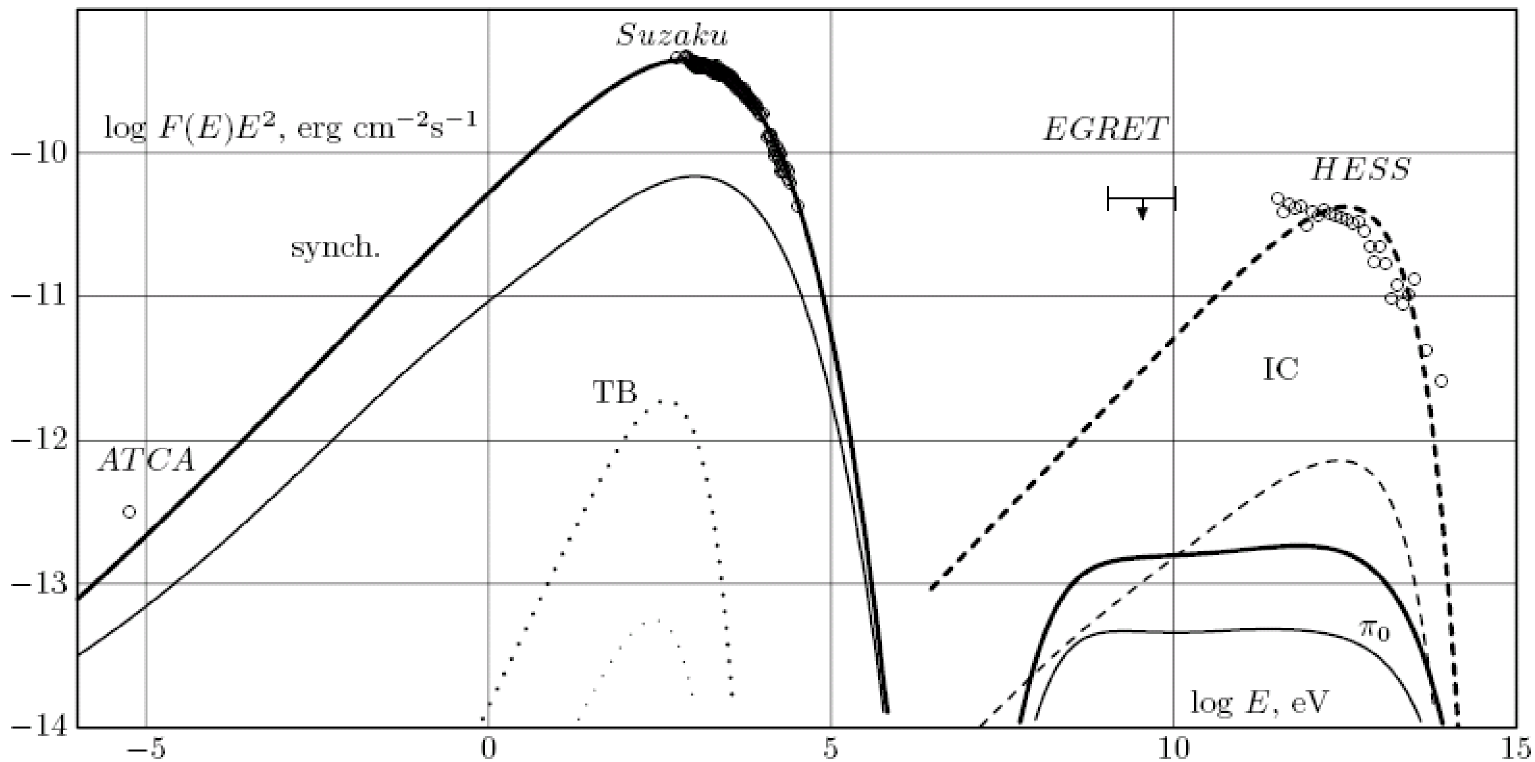

Fig. 8.— Broad-band emission of RX J1713.7-3946 for the leptonic scenario of gamma-rays with a non-modified forward shock. The principal model parameters are: t = 1620 yr, D = 1.5 kpc, n_H =0.02 cm^{-3}, $E_{SN} = 1.2 \cdot 10^{51}$ erg, $M_{ej} = 0.74 M_{\odot}$, $M_A^f = 69$, $M_A^b = 10$, $\xi_0 = 0.1$, $K_{ep}^f = 2.3 \cdot 10^{-2}$, $K_{ep}^b = 9 \cdot 10^{-4}$. The calculations lead to the following values of the magnetic fields and the shock speeds at the present epoch: the magnetic field downstream of the forward and reverse shocks $B_f = 17$ μG and $B_b = 31$ μG, respectively, the speed of the forward shock V_f = 3830 km s^{-1}, the speed of the reverse shock V_b = −1220 km s^{-1}. The following radiation processes are taken into account: synchrotron radiation of accelerated electrons (solid curve on the left), IC emission (dashed line), gamma-ray emission from pion decay (solid line on the right), thermal bremsstrahlung (dotted line). The input of the reverse shock is shown by the corresponding thin lines.

Radial profiles

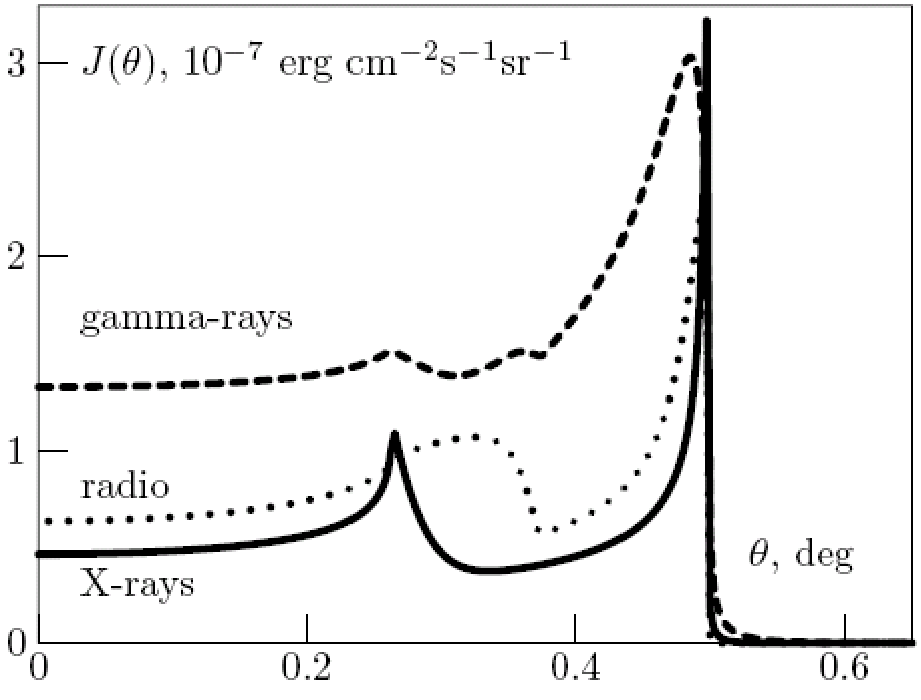

Fig. 10.— Radial profiles of 2 keV X-rays (multiplied to 0.04, solid line), 1 TeV gamma-ray emission (dashed line) and 1.4 GHz radio-emission (multiplied to 10^3, dotted line), calculated for the hadronic scenario in the uniform medium.

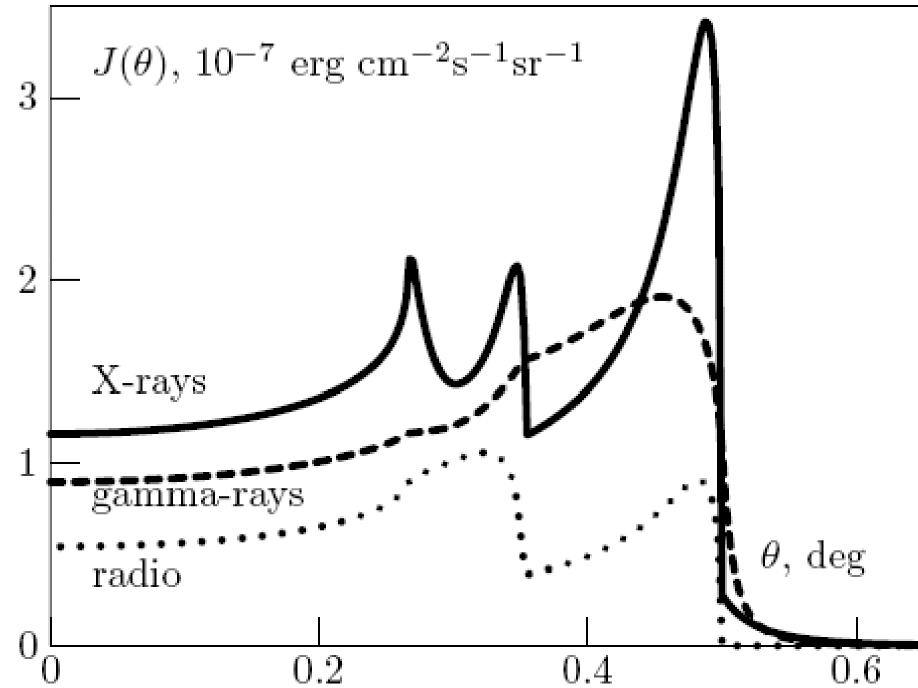

Fig. 11.— Profiles of 2 keV X-ray emission (multiplied to 0.1, solid line), 1 TeV gamma-emission (dashed line) and 1.4 GHz radio-emission (multiplied to 10^3, dotted line) for the leptonic scenario with the non-modified forward shock.

Comparison of hadronic and leptonic radial gamma-ray profiles

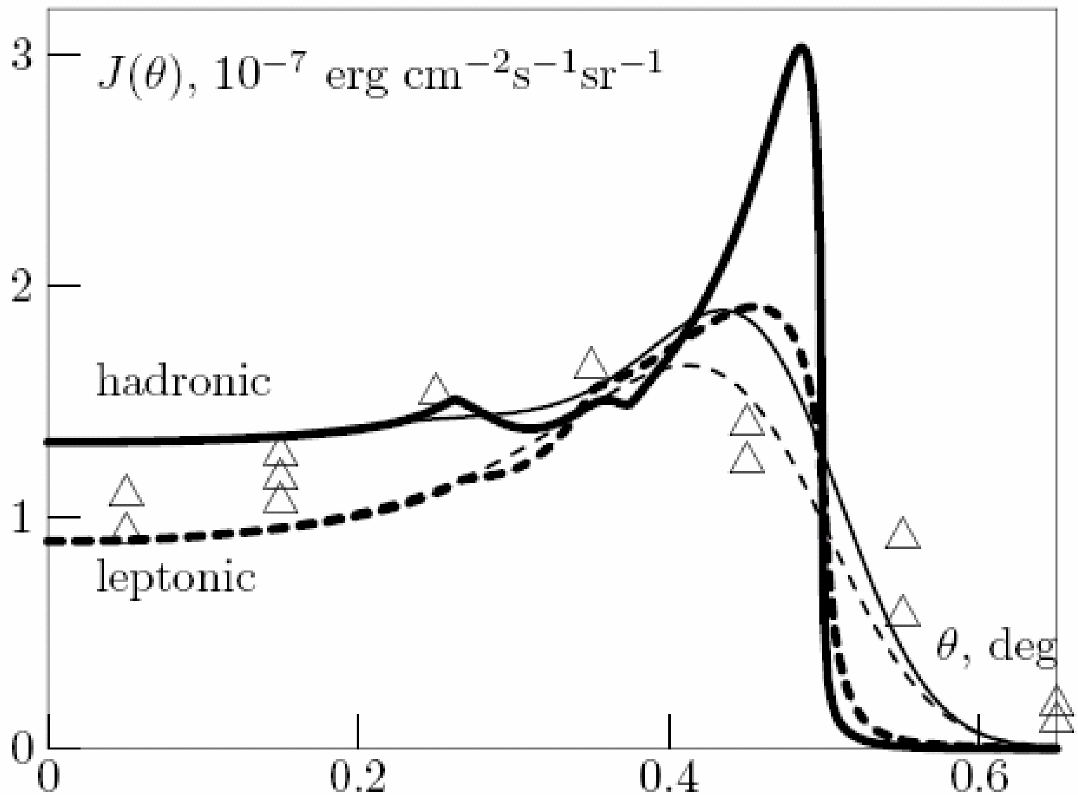

Fig. 13.— Radial Profiles of 1 TeV gamma-rays for the hadronic scenario in the uniform medium (solid) and for the leptonic scenario with the unmodified forward shock (dashed). The profiles smoothed with a Gaussian point spread function with $\sigma = 0.05°$ are also shown (thin lines). The triangles show the azimuthally averaged TeV gamma-ray radial profile observed by HESS (Aharonian et al. 2007a).

Composite model

Factor of 120 enhancement for clouds

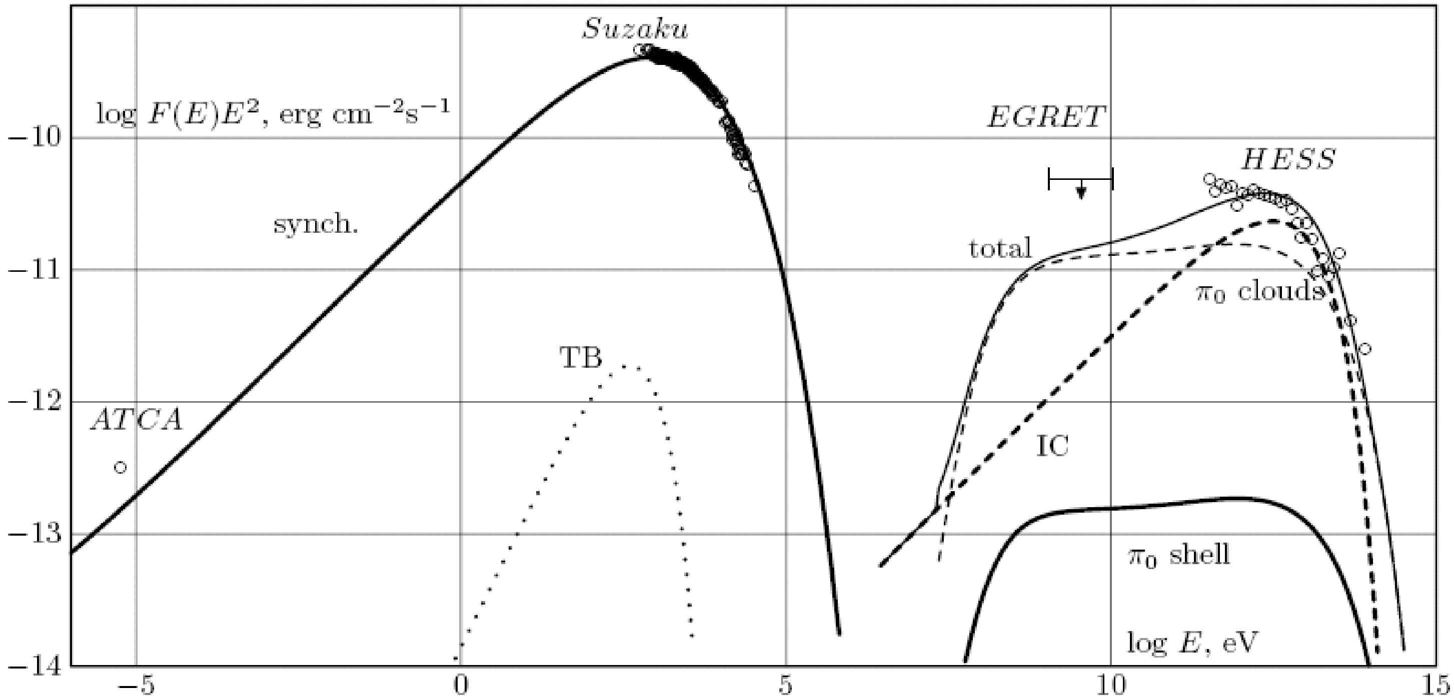

Fig. 14.— Broad-band emission of RX J1713.7-3946 for the composite scenario of gamma-rays with a non-modified forward shock and dense clouds. The principal model parameters are: $t = 1620$ yr, $D = 1.5$ kpc, n_H =0.02 cm^{-3}, $E_{SN} = 1.2 \cdot 10^{51}$ erg, $M_{ej} = 0.74 M_{\odot}$, $M_A^f = 55$, $M_A^b = 10$, $\xi_0 = 0.1$, $K_{ep}^f = 1.4 \cdot 10^{-2}$, $K_{ep}^b = 9 \cdot 10^{-4}$. The calculations lead to the following values of the magnetic fields and the shock speeds at the present epoch: the magnetic field downstream of the forward and reverse shocks $B_f = 22$ μG and $B_b = 31$ μG, respectively, the speed of the forward shock $V_f = 3830$ km s^{-1}, the speed of the reverse shock $V_b = -1220$ km s^{-1}. The following radiation processes are taken into account: synchrotron radiation of accelerated electrons (solid curve on the left), thermal bremsstrahlung (dotted line), IC gamma-ray emission of the entire remnant including forward and reverse shocks (dashed line), hadronic component of gamma-rays from the remnant's shell (solid line on the right) as well as from dense clouds assuming the factor of 120 enhancement of the flux (thin dashed line). We also show the total gamma-ray emission from the entire remnant including the dense clouds (thin solid line).

Summary

1. The current RS position in RX J1713.7-3946 corresponds to the Ib/c or IIb supernova explosion with a low ejected mass (<2 solar masses).
2. Both the leptonic and the hadronic origin of gamma-emission of complex SNR RX J1713 are possible.
3. The spectral shape of gamma-ray spectra is better reproduced in the hadronic model.
4. In the hadronic model the following conditions must be satisfied:

a) SNR shock must be significantly modified throughout all surface in order to suppress thermal X-rays and to produce enough pion-decay gamma-rays.

b) The line X-ray emission of heavy ions must be suppressed due to a low metallicity or an unusual ionization state of the plasma downstream of the forward shock.

c) If the forward shock interacts with clouds C and D the penetration of high-energy particles into the clouds must be suppressed.

d) The absence of the sharp X-ray filament at the remnant periphery should be explained (nonuniform circ. medium?)

5. If the inner ring is indeed a reverse shock, its proper motion in the direction to the center of the SNR can be measured (1-10 thousand km/s depending on the density distribution in the circ. medium).